

**An HNCA Pulse Scheme for the Backbone Assignment of  $^{15}\text{N}$ ,  $^{13}\text{C}$ ,  $^2\text{H}$ -Labeled Proteins: Application to a 37-kDa *Trp* Repressor-DNA Complex**

Toshio Yamazaki,<sup>†</sup> Weontae Lee,<sup>‡</sup> Matthew Revington,<sup>‡</sup> Debra L. Mattiello,<sup>§</sup> Frederick W. Dahlquist,<sup>||</sup> Cheryl H. Arrowsmith,<sup>‡</sup> and Lewis E. Kay\*,<sup>†</sup>

*Protein Engineering Centers of Excellence and Departments of Medical Genetics, Biochemistry, and Chemistry, University of Toronto  
Toronto, Ontario, Canada M5S 1A8  
Division of Molecular and Structural Biology  
Ontario Cancer Institute and  
Department of Medical Biophysics, University of Toronto  
500 Sherbourne Street, Toronto, Ontario, Canada M4X 1K9  
Varian Associates, 3120 Hansen Way  
Palo Alto, California 94304  
Institute of Molecular Biology and  
Department of Chemistry, University of Oregon  
Eugene, Oregon 97403-1229*

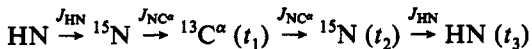
Received March 31, 1994

The development of multidimensional triple-resonance NMR spectroscopy has had a significant impact on solution structure studies of proteins with molecular masses less than approximately 20 kDa.<sup>1,2</sup> For many proteins in this molecular mass range the transfer of magnetization between nuclei via scalar couplings is sufficiently rapid, relative to the decay of magnetization via relaxation, that high-sensitivity spectra can be recorded. However, the rate of magnetization decay increases as a function of the molecular weight of the protein under study so that for molecules with molecular masses in excess of  $\sim$ 20–25 kDa many of the present experiments may fail. An attractive approach to increasing the molecular mass limitations of the current methods is to decrease the efficiency of  $^{13}\text{C}$  relaxation through the use of deuteration. Because the gyromagnetic ratio of  $^2\text{H}$  is roughly a factor of 7 lower than that of  $^1\text{H}$ , a significant decrease in the carbon relaxation rate is anticipated; the dipolar contribution of a deuteron to the line width of a  $^{13}\text{C}$  spin attached to a molecule undergoing isotropic motion with a correlation time of 15 ns is  $\sim$ 1.5 Hz as compared with  $\sim$ 20 Hz for the case of a  $^{13}\text{C}$ – $^1\text{H}$  pair. Recently Bax and co-workers have reported a triple-resonance 4D experiment connecting sequential amides in  $^2\text{H}$ ,  $^{13}\text{C}$ ,  $^{15}\text{N}$ -enriched proteins which employs  $^2\text{H}$  decoupling during periods when carbon transverse magnetization is present to eliminate the effects of scalar relaxation of the second kind introduced by deuteration.<sup>3</sup> These authors have also shown resolution and sensitivity benefits in 2D H(N)CA spectra of 85%-deuterated calcineurin relative to spectra recorded on the fully protonated molecule.<sup>3</sup> Kushlan and LeMaster have also demonstrated resolution and sensitivity enhancements in heteronuclear spectra of [50%-U- $^2\text{H}$ , 2- $^{13}\text{C}$ ]glycine-labeled *Escherichia coli* thioredoxin.<sup>4</sup>

An important experiment in the backbone assignment of  $^{15}\text{N}$ ,  $^{13}\text{C}$ -labeled proteins is the HNCA,<sup>5,6</sup> which provides both intra- and inter-residue correlations. A significant limitation of the experiment, however, is the poor resolution in the  $^{13}\text{C}^\alpha$  dimension, in large part due to the limited acquisition time that

can be allowed for carbon evolution as a result of homonuclear carbon–carbon couplings and short transverse relaxation times. The use of a  $^{15}\text{N}$ ,  $^{13}\text{C}$ ,  $^2\text{H}$ -labeled protein in concert with constant time carbon evolution<sup>7,8</sup> with  $^2\text{H}$  decoupling during this period<sup>3,4,9</sup> can result in significant improvements in resolution relative to the present implementation of the experiment. In this communication, a constant time HNCA experiment is presented which provides high resolution in both carbon and nitrogen indirectly detected dimensions. Using this experiment we have obtained 100% of the intra-residue and 94% of the inter-residue correlations involving backbone  $^{13}\text{C}^\alpha$ ,  $^{15}\text{N}$ , and HN chemical shifts of a 37-kDa ternary complex of  $^2\text{H}$ ,  $^{13}\text{C}$ ,  $^{15}\text{N}$ -labeled *trp* repressor, a 20 base pair *trp* operator DNA sequence, and the corepressor, 5-methyltryptophan.

Figure 1 illustrates the pulse sequence that has been employed. Details of HNCA pulse schemes that do not employ constant time evolution in the carbon dimension and other very similar pulse sequences can be found in the literature, and therefore only a summary of the salient features of the present experiment will be presented here. The flow of magnetization can be described by



with the relevant couplings involved in each magnetization transfer step indicated above the arrows;  $t_1$ ,  $t_2$ , and  $t_3$  denote acquisition times. Note that the constant time delay,  $2T_C$ , during which the  $^{13}\text{C}$  chemical shift is recorded is set to  $1/(J_{\text{CC}})$  where  $J_{\text{CC}}$  is the one-bond carbon–carbon coupling.<sup>7,8</sup> Briefly, the scheme makes use of gradients (i) to select for the coherence transfer pathway passing through nitrogen using an enhanced sensitivity approach described previously<sup>10,11</sup> and (ii) to minimize both the artifact content and the residual water in the spectrum.<sup>12,13</sup> In addition, dephasing of water is minimized in the experiment, in part by restoring the water magnetization to the  $+z$  axis prior to detection.<sup>14,15</sup> This is accomplished by making use of a water selective 90° pulse applied at point a in the sequence which restores the water magnetization to the  $+z$  axis and ensuring that prior to the application of  $^1\text{H}$  decoupling at points b and d in the sequence the water magnetization is rotated so as to be colinear with the WALTZ decoupling field and subsequently rotated back to the  $z$  axis at the termination of decoupling.<sup>15</sup>

For the majority of residues in large proteins ( $>\sim$ 20 kDa) relaxation during the  $2T_C$  constant time period greatly attenuates or eliminates signals from proton-bearing  $^{13}\text{C}^\alpha$  spins. However, in regions of the molecule with significant mobility this may not be the case, and for fractionally deuterated protein samples this gives rise to two sets of peaks for each residue arising from  $^{13}\text{C}^\alpha$  spins one-bond coupled to either  $^1\text{H}$  or  $^2\text{H}$ . Because of the substantial one-bond  $^2\text{H}$  isotope shift ( $\sim$ 0.4 ppm), the doubling

- (7) Santoro, J.; King, G. C. *J. Magn. Reson.* 1992, 97, 202.
- (8) Vuister, G. W.; Bax, A. *J. Magn. Reson.* 1993, 101, 201.
- (9) Browne, D. T.; Kenyon, G. L.; Packer, E. L.; Sternlicht, H.; Wilson, D. M. *J. Am. Chem. Soc.* 1973, 95, 1316.
- (10) Kay, L. E.; Keiffer, P.; Saarinen, T. *J. Am. Chem. Soc.* 1992, 114, 10663.
- (11) Muhandiram, D. R.; Kay, L. E. *J. Magn. Reson., Ser. B* 1994, 103, 203.
- (12) Hurd, R. E.; John, B. K. *J. Magn. Reson.* 1991, 91, 648.
- (13) Bax, A.; Pochapsky, S. *J. Magn. Reson.* 1992, 99, 638.
- (14) Grzesiek, S.; Bax, A. *J. Am. Chem. Soc.* 1993, 115, 12593.
- (15) Kay, L. E.; Xu, G. Y.; Yamazaki, T. *J. Magn. Reson.* in press.
- (16) McCoy, M.; Mueller, L. *J. Am. Chem. Soc.* 1992, 114, 2108.
- (17) Shaka, A. J.; Keeler, J.; Frenkel, T.; Freeman, R. *J. Magn. Reson.* 1983, 52, 335.
- (18) McCoy, M.; Mueller, L. *J. Magn. Reson.* 1992, 98, 674.
- (19) Marion, D.; Ikura, M.; Tschudin, R.; Bax, A. *J. Magn. Reson.* 1989, 85, 393.
- (20) Paulh, J. L.; Yanofsky, C. *Nucleic Acids Res.* 1986, 14, 7851.
- (21) Arrowsmith, C. H.; Patcher, R. B.; Altman, R. B.; Iyer, S. B.; Jardetzky, O. *Biochemistry* 1990, 29, 6332.
- (22) Delaglio, F. *NMRPipe* System of Software (Bethesda, Maryland: National Institutes of Health).
- (23) Zhu, G.; Bax, A. *J. Magn. Reson.* 1990, 90, 405.

\* Protein Engineering Centers of Excellence and Departments of Medical Genetics, Biochemistry, and Chemistry, University of Toronto.

<sup>†</sup> Division of Molecular and Structural Biology, Ontario Cancer Institute and Department of Medical Biophysics, University of Toronto.

<sup>‡</sup> Varian Associates.

<sup>§</sup> Institute of Molecular Biology and Department of Chemistry, University of Oregon.

(1) Bax, A.; Grzesiek, S. *Acc. Chem. Res.* 1993, 26, 131.

(2) Clore, G. M.; Gronenborn, A. *Science* 1991, 252, 1391.

(3) Grzesiek, S.; Angliister, J.; Ren, H.; Bax, A. *J. Am. Chem. Soc.* 1993, 115, 4369.

(4) Kushlan, D. M.; LeMaster, D. M. *J. Biomol. NMR* 1993, 3, 701.

(5) Ikura, M.; Kay, L. E.; Bax, A. *Biochemistry* 1990, 29, 4659.

(6) Kay, L. E.; Ikura, M.; Tschudin, R.; Bax, A. *J. Magn. Reson.* 1990, 89, 496.

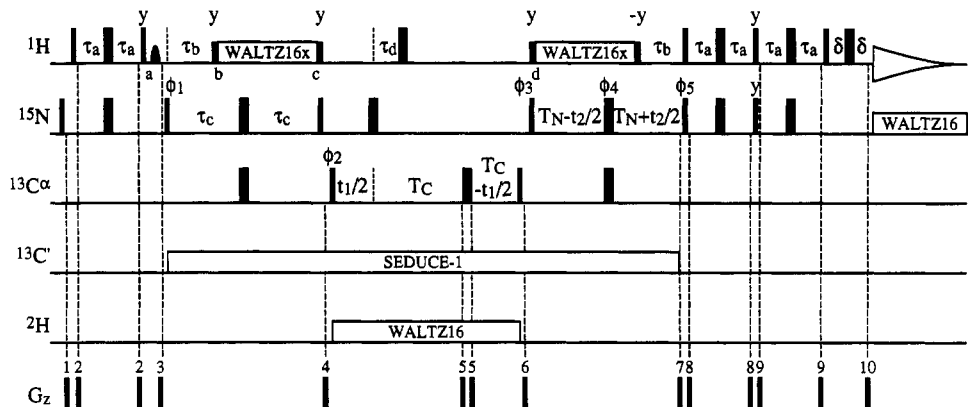


**Figure 1.** Pulse scheme of the constant time HNCA experiment. All narrow (wide) pulses are applied with a flip angle of  $90^\circ$  ( $180^\circ$ ). Unless indicated otherwise, pulses are applied along the  $x$  axis. The carriers are centered at 4.7 (water), 119, 58, and 4.5 ppm for  $^1\text{H}$ ,  $^{15}\text{N}$ ,  $^{13}\text{C}$ , and  $^2\text{H}$ , respectively. Proton pulses are applied using a 23-kHz field, with the exception of the selective water pulse at point a, which is a 2-ms  $90^\circ$  pulse with a SEDUCE-1<sup>16</sup> profile (270-Hz field at peak height) and the  $90^\circ_{\pm y}$  pulses flanking the WALTZ-16<sub>x</sub><sup>17</sup> decoupling intervals which are applied using a 6.8-kHz field.  $^1\text{H}$  WALTZ decoupling is achieved using a 6.8-kHz field. High-power  $^{15}\text{N}$  pulses are applied using a 4.3-kHz field with 1-kHz  $^{15}\text{N}$  decoupling during acquisition. The  $^{13}\text{C}^\alpha$  pulses are applied with an 18-kHz field, while  $^{13}\text{C}^\beta$  decoupling is achieved using a cosine modulated WALTZ-16 field employing pulses having the SEDUCE-1 profile<sup>18</sup> (330- $\mu\text{s}$   $90^\circ$  pulse). All carbon pulses (including SEDUCE decoupling) were applied using only a single channel.  $^2\text{H}$  decoupling, applied with rf generated from a separate synthesizer, was achieved using an 850-Hz WALTZ field. The delays employed are as follows:  $\tau_a = 2.3$  ms,  $\tau_b = 5.5$  ms,  $\tau_c = 11.0$  ms,  $\tau_d = 1.7$  ms,  $T_c = 13.3$  ms,  $T_N = 12.4$  ms,  $\delta = 0.5$  ms. The phase cycling employed is as follows:  $\phi_1 = (x, -x)$ ;  $\phi_2 = 2(x), 2(-x)$ ;  $\phi_3 = x$ ;  $\phi_4 = 4(x), 4(-x)$ ;  $\phi_5 = x$ ;  $\text{rec} = (x, -x, -x, x)$ . Quadrature in  $F_1$  is obtained via States-TPPI<sup>19</sup> of  $\phi_2$ . For each value of  $t_2$ , N- and P-type coherences are obtained by recording two data sets where the sign of the gradient  $g_7$  is inverted and  $180^\circ$  added to the phase  $\phi_5$  for the second data set. The phase  $\phi_3$  is incremented by  $180^\circ$  along with the phase of the receiver for each  $t_2$  increment. The durations and strengths of the gradients are as follows:  $g_1 = (0.5$  ms, 8 G/cm),  $g_2 = (0.5$  ms, 4G/cm),  $g_3 = (1.0$  ms, 10 G/cm),  $g_4 = (1.0$  ms, -5 G/cm),  $g_5 = (0.1$  ms, 20 G/cm),  $g_6 = (0.6$  ms, 10 G/cm),  $g_7 = (1.25$  ms, 30 G/cm),  $g_8 = (0.5$  ms, 8 G/cm),  $g_9 = (0.3$  ms, 2 G/cm),  $g_{10} = (0.125$  ms, 27.8 G/cm). Decoupling is interrupted during the application of gradient pulses.

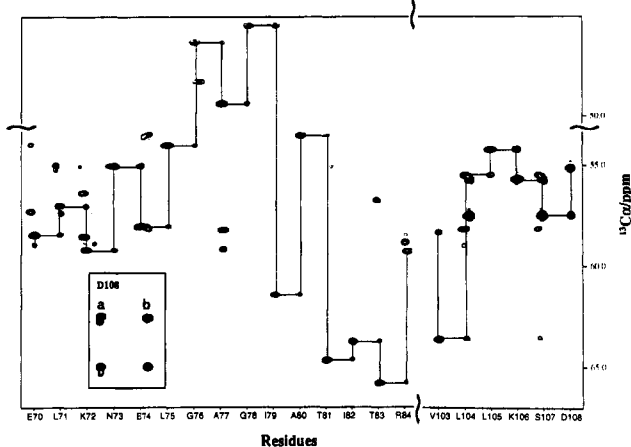


**Figure 2.** Strip plot displaying the sequential connectivities for the helix-turn-helix DNA binding region (residues 70–84) and a portion of helix F (residues 103–108) of the ternary complex of  $^{15}\text{N}$ ,  $^{13}\text{C}$ ,  $^2\text{H}$ -labeled *trp* repressor, 5-methyltryptophan, and a palindrome 20 base pair *trp* operator DNA sequence (total molecular mass of 37 kDa). The labeled protein was isolated from *E. coli* strain CY15070 grown on  $^{15}\text{N}$ ,  $^{13}\text{C}$ -labeled M9 media with 69%  $^2\text{H}_2\text{O}$ /31%  $^1\text{H}_2\text{O}$  as described previously.<sup>20,21</sup> The data set was recorded as an  $84 \times 28 \times 512$  complex matrix with acquisition times of  $t_1(^{13}\text{C}) = 25.7$  ms,  $t_2(^{15}\text{N}) = 23.0$  ms,  $t_3(^1\text{H}) = 64.0$  ms, relaxation delay 2 s, 8 transients/FID. The total recording time was 44 h. The data set was processed using nmrPipe/nmrDraw software developed by F. Delaglio at the NIH.<sup>22</sup> In order to improve resolution in  $F_1$ , mirror image linear prediction was employed<sup>23</sup> prior to zero filling in this dimension. The size of the absorptive part of the final 3D spectrum was  $256 \times 64 \times 512$ . The glycine resonances are negative due to the use of a constant time carbon evolution period of  $1/J_{\text{CC}}$ . The inset in the lower left-hand corner shows the intra- (upper) and inter-residue cross peaks for D108 using the pulse scheme in Figure 1 where in column a a  $^1\text{H}$  decoupling between points c and d in Figure 1 replaces the  $^1\text{H}$   $180^\circ$  pulse and in column b the scheme of Figure 1 has been employed.

of signals that results may complicate data interpretation. The suppression of signals arising from the population of  $^{13}\text{C}^\alpha$  spins that are one-bond coupled to  $^1\text{H}$  as opposed to  $^2\text{H}$  is achieved in the present scheme by ensuring that evolution due to  $^1\text{H}$ – $^{13}\text{C}$

couplings proceeds for a time  $2\tau_d = 1/(2J_{\text{CH}})$  between points c and d. Carbon magnetization arising from  $^{13}\text{C}^\alpha$ – $^1\text{H}^\alpha$  pairs is subsequently antiphase and is not refocused into an observable signal by the remaining pulses. Because carbon evolution due to long-range  $^1\text{H}$ – $^{13}\text{C}$  scalar couplings proceeds for only  $2\tau_d$  as well, these effects are negligible.

The experiment was conducted on a Varian UNITY 500 MHz spectrometer equipped with a pulsed field gradient unit and an actively shielded triple-resonance probe head. A single channel was used for the  $^{15}\text{N}$  pulses/decoupling as well as  $^2\text{H}$  decoupling, requiring a number of small modifications to our spectrometer. The  $^2\text{H}$  lock receiver was not disabled during either application of gradients or  $^2\text{H}$  decoupling. A 3D data set was recorded on a 1.2 mM uniformly  $^{15}\text{N}$ ,  $^{13}\text{C}$ , ~70%  $^2\text{H}$  labeled *trp* repressor dimer complexed with unlabeled 5-methyltryptophan and a 20 base pair DNA fragment corresponding to the *trp* operator.

Figure 2 illustrates a strip display of the connectivities obtained for the helix-turn-helix DNA binding region (residues 75–84) and a portion of helix F (residues 103–108) of the *trp* repressor dimer. The excellent resolution in the carbon dimension, in particular, enables the assignment of large stretches of the backbone of the protein, despite the predominantly  $\alpha$ -helical secondary structure of the protein. The inset to Figure 2 shows a comparison of correlations involving D108 obtained using sequences where signals from  $^{13}\text{C}^\alpha$ – $^1\text{H}^\alpha$  pairs are not (a) or are (b) eliminated.

In this communication we have presented a constant time HNCA experiment which exploits the line-narrowing effects of deuteration to maximize both sensitivity and resolution. The high quality of the data obtained on a 37-kDa complex in under 2 days of recording time suggests that the use of deuteration in concert with  $^{15}\text{N}$ ,  $^{13}\text{C}$  labeling may prove to be an important strategy in extending the molecular weight limitations of current NMR techniques.

**Acknowledgment.** The authors are grateful to Dr. George Gray, Varian Inc., for recording preliminary experiments. This research was supported by the National Cancer Institute of Canada (C.H.A and L.E.K), by the Human Frontier Science Program (C.H.A), and by a Public Health Service Grant (AI 17807) from the National Institutes of Health (F.W.D). T.Y is the recipient of a Human Frontiers Science Program Fellowship.